# analytical chemistry

Article

pubs.acs.org/ac

Raman Thermometry in Water, Ethanol, and Ethanol/Nitrogen Mixtures from Ambient to Critical Conditions

Tobias C. Klima and Andreas S. Braeuer*

Institute of Thermal-, Environmental-, and Resources' Process Engineering (ITUN), Technische Universität Bergakademie Freiberg (TUBAF), 09599 Freiberg, Germany

Ⓢ Supporting Information

ABSTRACT: We present investigations into remote liquid temperature sensing with Raman spectroscopy using different evaluation methods for the OH stretching vibration band. Water, ethanol, and ethanol saturated with nitrogen, all as liquids or liquid-like supercritical fluids, are pumped through a heated microcapillary system at elevated pressures. Raman spectra are recorded from the liquid inside the microcapillary and are evaluated with respect to the temperature sensitivity of the OH stretching vibration. The four approaches applied are (i) to evaluate the center position of the Raman OH-band, (ii) the integrated absolute difference spectrum, (iii) the intensity ratio of two regions of the OH-band, and (iv) the intensity ratio of two fitted Gaussian peaks. The temperature range investigated covers from ambient temperature to the component's respective boiling temperature or critical temperature at sub- and supercritical pressures. Precision and robustness of the employed methods are characterized. It is shown that two out of the four methods feature temperature deviations smaller than 5 K at all pressures and that one method can also be applied to liquid mixtures of ethanol and nitrogen. Applicability to other liquids and mixtures is discussed.
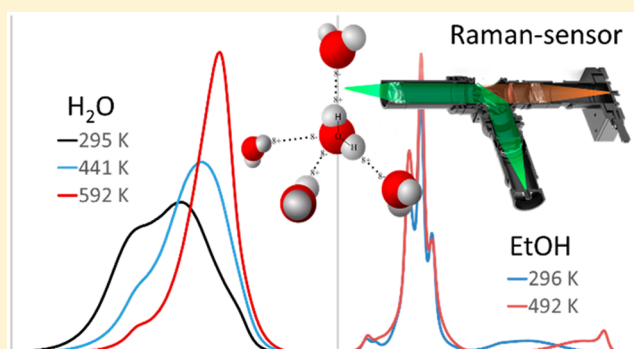
Whenever it has to be assured that the action of measuring temperature does not disturb the system from which the temperature should be sensed, remote thermometry strategies are the first choice. This can be, for example, in spray research when a physical temperature probe would invade into the flow and into the heat and mass transfer processes going on in the spray. Similar examples can be found in different kinds of reacting or nonreacting flows. Therefore, the provision of optical measurement techniques for the remote and noninvasive measurement of temperature is essential for analyzing, understanding and controlling a variety of operations in process technology.

Out of the numerous methods for fluid thermometry,[1,2] spontaneous Raman spectroscopy is one that does not rely on the addition of a temperature indicator and thus can provide spatially and temporally resolved temperature from the unspoiled fluid itself. The extraction of temperature from a Raman spectrum can be based on different temperature sensitive features of an assemblage of molecules that are reflected in the Raman spectrum. This can be (i) the temperature sensitive occupation distribution across energy levels (rotational Raman thermometry[3−5] vibrational Raman thermometry including Q-branch Raman thermometry,[6] hot-band Raman thermometry,[7] and Stokes/anti-Stokes Raman thermometry,[8] or (ii) the temperature sensitive development of a hydrogen bonding network. The temperature sensitive development of hydrogen bonds has been analyzed from the point of physical chemistry[9−12] and has been exploited for

remote Raman thermometry in water,[13,14] ammonia,[15] and alcohol[16,17] containing systems. The temperature sensitive development of hydrogen bonds influences the eigenfrequency of the intramolecular Raman active vibrations between the nuclei that are involved in the hydrogen bonding network. These are the symmetric stretching vibration and the bending vibration of water and the stretching vibration of the hydroxyl group of alcohols, whose eigenfrequencies in a system containing hydrogen bonds are broadly distributed and on average less than in a not hydrogen bonded system. For example, the symmetric water stretching vibration of water vapor (no hydrogen bonds) results in a distinct, sharp peak at a Raman-shift of 3650 cm^{-1}, while that of liquid water (hydrogen bonds) forms a broad Raman band at Raman-shifts between 3000 and 3800 cm^{-1}. We refer to the symmetric stretching vibration of water and to the stretching vibration of alcohols as OH stretching vibration and to its resulting Raman spectrum as the Raman OH-band. According to literature, one can find different correlations between the temperature sensitive development of hydrogen bonds and the different characteristics of the OH stretching vibration Raman signal. Some correlations divide the Raman OH-band into portions and consider their temperature sensitive ratio/distribu-

tion[16,18,19] Other correlations consider the temperature sensitive shift of the central band position or of the centroid of the band,[20] and still others are based on contour fits or indirect hard modeling methods[21]

For Raman thermometry applications, these correlations have (i) never been analyzed at elevated pressure, which significantly extends the temperature range at which alcohols or water are still in the liquid state and (ii) seldom for mixtures instead of pure compounds.

We here report four different approaches of correlating the Raman OH-band of water, ethanol, and a mixture of ethanol and nitrogen with the temperature in the temperature range from room temperature to the critical temperature.

■ EXPERIMENTAL SECTION

Instrumentation. The experimental setup is schematically depicted in Figure 1. Water or ethanol are continuously fed in
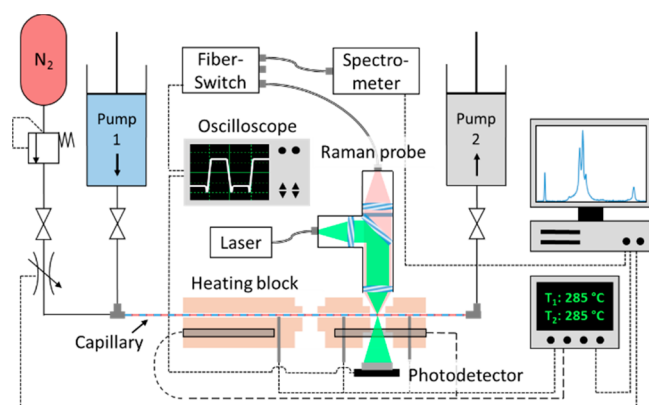
Figure 1. Schematic overview of the experimental setup.

controlled flow rates to the setup via a high precision high pressure syringe pump (labeled "pump 1"). At a T-junction, the liquid flow can be mixed with defined amounts of gaseous nitrogen fed via a mass flow controller. From this junction on, the fluid stream runs through a microcapillary (labeled "capillary") with an inner diameter of 300 μm and an outer diameter of 800 μm made out of fused silica. Both gas and liquid feed can be varied independently, allowing for mixture compositions from pure ethanol or water to pure nitrogen. The glass capillary is set in a steel block (labeled "heating block") of 300 mm length with four heating cartridges inserted horizontally and symmetrically placed. Two of these are depicted in Figure 1, as well as three of the six type K thermocouples equidistantly placed along the capillary to monitor the temperature (up to 700 ± 0.2 K), set vertically in the block. Access holes drilled into the steel block allow for optical access (two of five shown), and thus the acquisition of Raman spectra by the Raman probe. For better understanding of the layout of the heating block, Figure 2 shows a sectional rendered image. Downstream of the steel block, another high pressure pump (labeled "pump 2") is operated in reverse mode to receive the fluid and control the pressure of the system at pulsation free conditions up to 30 MPa.

If the fed flow rates result in a mixture composition located in the miscibility gap, the flow in the glass capillary will separate in alternating liquid phase and vapor phase segments in a harmonic pattern (picture in Figure 3). The fluid segments have a length of typically 2 mm, and thus a high surface
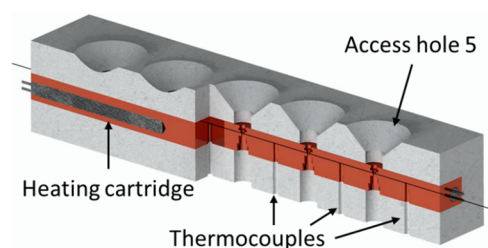
Figure 2. Rendered sectional image of the heating block with heating cartridge, thermocouples, and access hole pointed out.


Figure 3. Picture of the segmented flow in the glass capillary.

compared to their volume; furthermore, the radial surface is high compared to their volume. Heat and mass transfer processes have thus only to overcome short characteristic lengths. This results in extremely fast establishment of thermodynamic equilibrium while the fluid accommodates to the temperature of the steel block almost immediately while propagating through it. This means the liquid segments are saturated even at high temperatures in the measurement position (as long as the two-phase flow persists), and measurements in saturated liquid phases are possible.

Via the optical access located furthest downstream, Raman spectra are recorded from the fluids inside the capillary. The excitation source is a continuous wave laser operating at 150 mW at 532 nm. The Raman signals are excited and acquired in backscattering configuration by the Raman probe shown in Figure 1 and spectrally resolved and quantified with a fiber-coupled spectrometer. When measuring in pure liquids, i.e., the fluid is in single phase, Raman spectra can easily be detected by applying 4 s integration time. In a segmented two-phase flow, this would result in superposition of signal originating from both phases. To discriminate between the two phases, and render phase-selective measurements possible, a photodetector is placed beneath the measurement position. This photo-electric guard detects the light of the laser passing through the capillary, varying in intensity with the current state of phase of the fluid in the measurement position. The resulting voltage signal outlined on the oscilloscope in Figure 1 allows for discrimination between vapor and liquid phase and consequently triggering the acquisition of Raman spectra of the desired phase. When the voltage signal on the oscilloscope indicates the start of a fluid segment of the desired phase to be measured, a trigger is sent to the fiber-switch shown in Figure 1 between the Raman probe and spectrometer. This fiber-switch directs the signal from the Raman probe to the spectrometer for a defined duration and switches the signal path to a signal dump afterward. A harmonic pattern of fluid segments and a stationary flow are crucial for this method to work. When the oscilloscope detects the arrival of the next fluid segment of the desired phase, the signal path is switched back to the spectrometer. Thus, the spectrometer can accumulate signal for 4 s continuously, while the signal will actually only arrive when the trigger system allows it. Typically, the frequency of segment passes of the same phase state is 3−6 Hz, and the trigger widths are set between 60 to 20 ms, respectively. From

these values, an effective integration time of approximately 0.5 s is calculated for the two-phase flow case.

Methods. We performed measurements with water at 0.5, 5, 10, 15, 20, 22.5, and 25 MPa, as well as with ethanol and ethanol saturated with nitrogen at 3, 5, 6, 6.5, and 8 MPa. After starting the fluid flow and setting the desired pressure, the temperature is increased in 10 K steps from ambient temperature to the fluid's boiling point or critical point (with respect to the set pressure). At each step, 32 spectra are recorded with 4 s integration time. The broad Raman OH-band of the spectra, stemming from the hydrogen bond network developed by water and ethanol, is evaluated due to its strong response to temperature variation. With increasing temperature, the intensities of the Raman OH-band at higher Raman-shifts increase, while the intensities at lower Raman-shifts decrease. Figuratively speaking, the Raman OH-band shifts weight to higher Raman-shifts, as is seen in Figure 4.
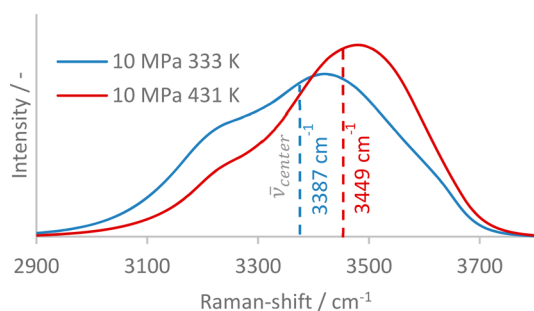
Figure 4. Raman OH-band of liquid water for 333 and 431 K at 10 MPa. The central Raman-shift $\overline{\nu}_{center}$ for each spectrum is given.

Four methods reported in the literature are applied and compared, each aiming to obtain a single value correlated with temperature from a spectrum. Each data point in the following figures represents the mean out of 32 measurements, and the error bars show the respective standard deviation.

Materials. Chemicals used in this work were: distilled water (T_c = 647 K, p_c = 22.1 MPa) according to ISO 3696 purchased form Kerndl, ethanol (T_c = 514 K, p_c = 6.14 MPa) with a purity of more than 99.9% purchased from Merck Millipore, and nitrogen (T_c = 126 K, p_c = 3.39 MPa) with more than 99.99% purity purchased from Praxair.

■ RESULTS AND DISCUSSION

OH$_{center}$ Method. The OH$_{center}$ method relies on the shift of the central Raman-shift $\overline{\nu}_{center}$ of the Raman OH-band to higher values with increasing temperature. This is shown for two example spectra from liquid water in Figure 4 at 10 MPa and 333 and 431 K. To calculate $\overline{\nu}_{center}$, the Raman OH-band is divided into two parts of equal integrated intensity, i.e., area. Figure 5 shows this correlation as the set system temperature T_{sys} over the respective central Raman-shift $\overline{\nu}_{center}$. The R^2 values greater 0.999 for all data sets indicate agreement of the fit equation and the experimental data. The equations fitted to the data in this work can be found in the Supporting Information.

One can use the fit functions for the computation of temperature T_{calc} as a function of the central Raman-shift $\overline{\nu}_{center}$ of the Raman OH-band. For water, the correlation between the set system temperature T_{sys} and the central Raman-shift $\overline{\nu}_{center}$ of the Raman OH-band is best described by a third-order polynomial function resulting in residuals $T_{calc} - T_{sys}$ smaller
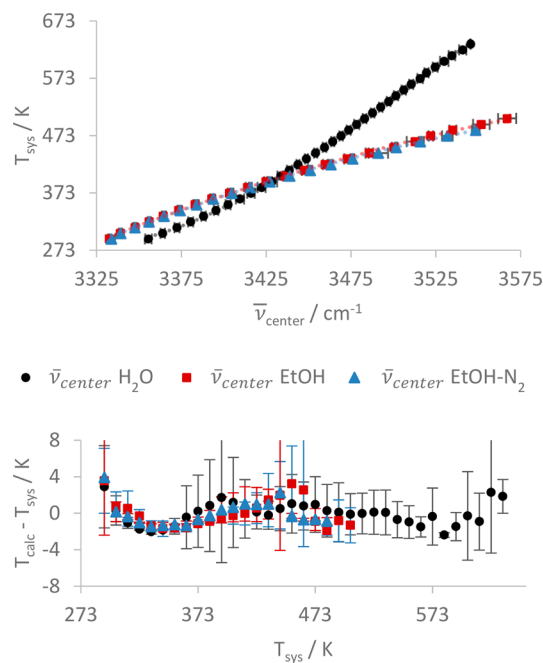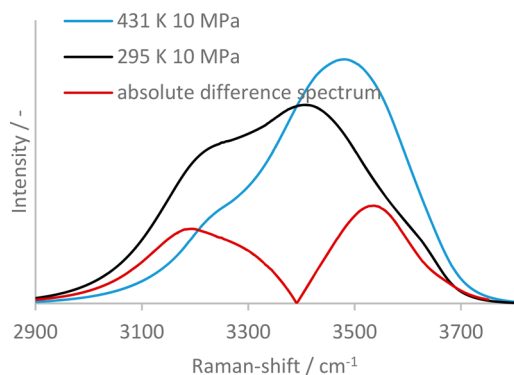

Figure 5. Top: Set system temperature T_{sys} as a function of the determined central Raman-shift $\overline{\nu}_{center}$ of the Raman OH-band for pure water, ethanol and ethanol saturated with nitrogen. Bottom: Difference of calculated temperature T_{calc} from set system temperature T_{sys}, when T_{calc} is computed according to the fit equations given in the top section of this figure.

than 5 K over the whole temperature range covered. Second-order polynomial fitting for water can be found in literature, however this only applies to temperature intervals smaller than 100 K. Both ethanol and ethanol-nitrogen can be adequately described by a second-order polynomial, yielding calculated temperatures T_{calc} with less than 5 K deviation from the set system temperature T_{sys} at all investigated temperatures. The correlations for pure ethanol and for the ethanol saturated with nitrogen are similar to each other. This is due to the rather small solubility of nitrogen in liquid ethanol (smaller than 4 mol % for all temperatures and pressures analyzed) and due to the little disturbance a dissolved nitrogen molecule causes to the hydrogen bonded network[22]

IADS Method. The integrated absolute difference spectrum (IADS) method evaluates the area normalized Raman OH-band with respect to an area normalized reference Raman OH-band taken at well-known conditions. The area normalized reference spectrum for water shown in Figure 6 was taken at 295 K and 10 MPa. Figure 6 shows that the absolute value of the difference between the area normalized reference Raman OH-band and the area normalized measured Raman OH-band is computed and provided as an absolute difference spectrum. As the shape of the Raman OH-band is a function of temperature, the absolute difference spectrum is also a function of temperature. Figure 7 correlates the set system temperature T_{sys} with the area under the absolute difference spectrum (integrated absolute difference IAD).

The R^2 values greater 0.9995 indicate agreement between the experimentally measured data points and the fit functions. For water, the correlation of the IAD and T_{sys} are fitted with a third-order polynomial, while the respective correlations are fitted with second-order polynomials for the systems containing pure ethanol or ethanol saturated with nitrogen.

Figure 6. Area normalized Raman OH-bands of a reference spectrum of water taken at 295 K and a measured spectrum of water taken at 431 K, both at 10 MPa, and their absolute difference spectrum.
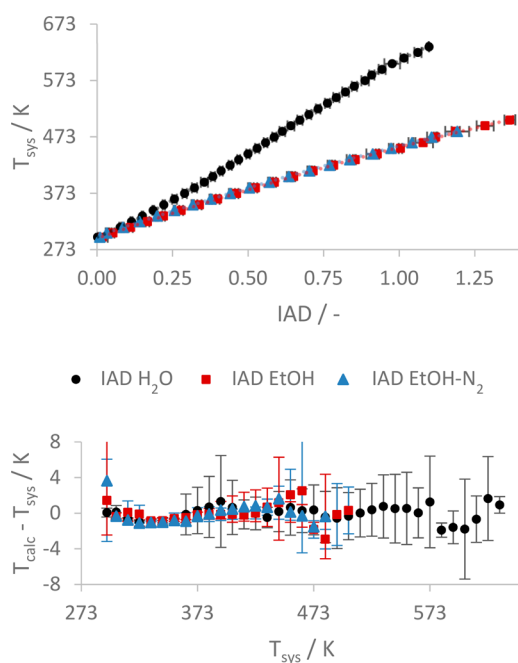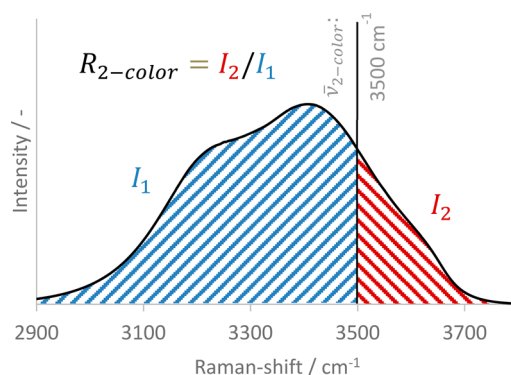

Figure 7. Top: Set system temperature T_{sys} as a function of integrated absolute difference (IAD) for pure water, ethanol, and ethanol saturated with nitrogen. Bottom: Difference of calculated temperature T_{calc} from set system temperature T_{sys}, when T_{calc} is computed according to the fit equations given in the top section of this figure.

According to the bottom part of Figure 7, the temperatures calculated from the obtained fit functions show precision far better than 5 K.

The difference between data from pure ethanol and the ethanol−nitrogen mixture appears to be even smaller compared to the OH_{center} method, stemming from an inherent correction mechanism of this method: The impact of dissolved nitrogen on the Raman OH-band in the case of the ethanol−nitrogen mixture is already accounted for by applying a reference spectrum from ethanol saturated with nitrogen.

Two-Color Method. The most straightforward method in this work is the two-color method. The spectrum is divided into two partial spectra at an arbitrary position $\overline{v}_{2\text{-color}}$, and each of the resulting partial spectra is integrated and the ratio $R_{2\text{-color}}$ of the integrals is calculated according to the equation inserted in Figure 8.

Figure 8. Raman OH-band of water at 295 K and 10 MPa with dividing position $\overline{v}_{2\text{-color}}$ The resulting partial spectra are colorized, and the equation for calculating the ratio of the integrated partial spectra is given.

The resulting ratio $R_{2\text{-color}}$ is correlated to the set system temperature T_{sys}, shown in Figure 9 The data for all three
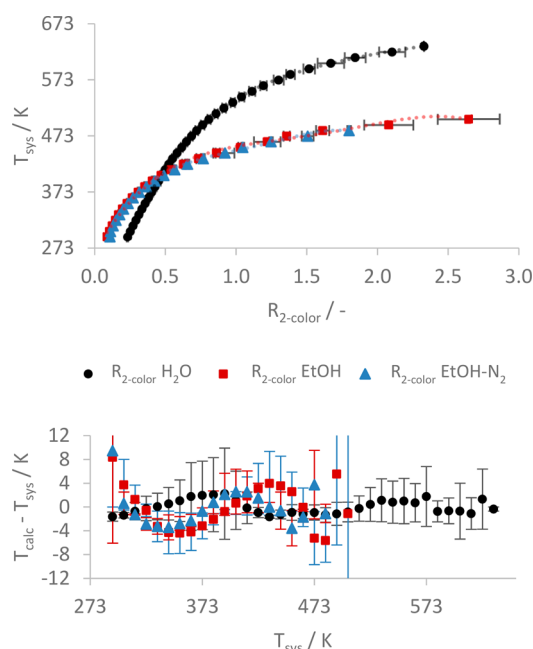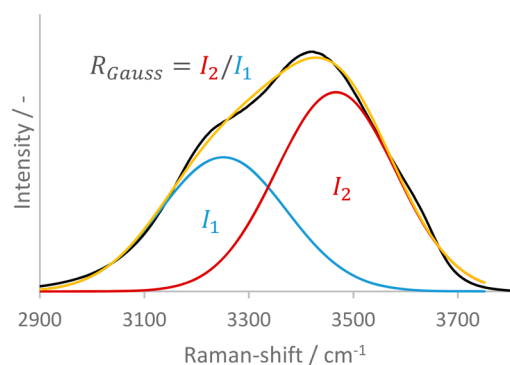

Figure 9. Top: Set system temperature T_{sys} as a function of 2-color ratio for pure water, ethanol, and ethanol saturated with nitrogen. Bottom: Difference of calculated temperature T_{calc} from set system temperature T_{sys}, when T_{calc} is computed according to the fit equations given in the top section of this figure.

systems are fitted by fourth-order polynomial functions. Even though lower orders are preferable, neither they nor any other function were found to describe the behavior adequately. The calculated temperatures show residuals $T_{calc} − T_{sys}$ from the set system temperature of up to 10 K. The location of the divider $\overline{v}_{2\text{-color}}$ has a large influence on the ratio $R_{2\text{-color}}$ and has to be chosen with care. It seems to be plausible to place the divider at the quasi-isosbestic point, i.e., the intersection of two spectra taken at consecutive temperatures 10 K apart to achieve a high variation with temperature. Unfortunately, this point is not at a constant position but instead shifts to larger Raman-shifts with increasing temperatures. Between 295 and 304 K, this point would lie at 3350 cm^{-1} yet between 592 and 601 K at 3515 cm^{-1}. When placing the divider at too small Raman-shifts, the

signal will occur almost completely to the right of the divider at high temperatures. The ratio of areas will then approach infinity. On the other hand, if the divider is placed at larger Raman-shifts, the gradient of the correlation at low temperatures is very steep, reducing the precision of the temperature determination in this temperature region tremendously. As a trade-off between these two scenarios, the divider $\bar{\nu}_{2\text{-color}}$ was positioned at 3500 cm^{-1} in this work.

Gauss Method. A method bearing some similarity to the 2-color method is the Gauss method, where the Raman OH-band is fitted by Gaussian peaks, and the ratio of the integrated intensities R_{Gauss} of these peaks acts as the value correlated with temperature. Here we use two Gauss peaks, while also more Gauss peaks can be used for fitting the Raman OH-band.[10] In Figure 10, an example water spectrum taken at 295 K and

Figure 10. Raman OH-band of water at 295 K and 10 MPa fitted by two Gaussian peaks with fitted envelope.

10 MPa with two fitted Gaussian peaks is shown as well as the resulting fitted envelope. The correlation of the set system temperature T_{sys} over R_{Gauss} in Figure 11 reveals the major
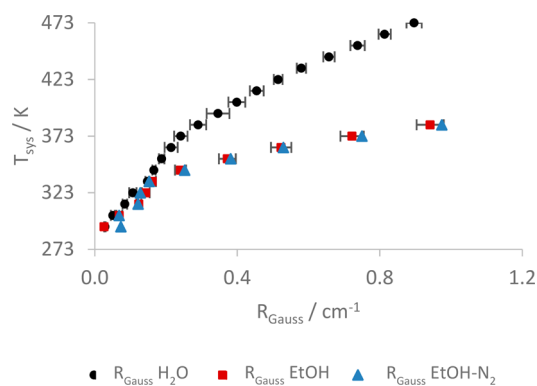
Figure 11. Set system temperature T_{sys} as a function of Gauss peak area ratios for water, pure ethanol, and ethanol saturated with nitrogen.

issue of this approach: The data up to a R_{Gauss} of 0.2 follow no mathematical function that could be fitted. This stems from the setup of the Gauss fitting algorithm, which can either allow for free movement of the peaks in terms of Raman-shift, or can fix the position of the Gaussians to a certain value. The first option means giving up uniqueness of the correlation because the same ratio may occur at different temperatures when the peaks do not change their area with temperature and simply are located at different Raman-shifts. Their ratio would then yield two possible temperature solutions when calculating T_{calc}.

The second option, keeping the peaks in place, is applicable over small temperature intervals, where the changes in the Raman OH-band are small enough to allow for satisfactory fitting by two Gaussians fixed in position. Considering the temperature ranges covered in this work, the approach fails; in extreme cases, one peak would be fitted with zero intensity and ratio calculation would thus become useless. For this reason, we abstained from fitting the data points and calculating temperatures based on the fits. Using more than two peaks for fitting the Raman OH-band reduces these problems but does not eliminate them[10]

Comparison of Methods. With the described inability of the Gauss method to yield a reliable fitted function over the complete temperature range, we omit this method from further considerations. For the other three methods, the mean absolute deviation $T_{\text{diff, system}}$ of the calculated temperature T_{sys} and system temperature T_{sys}, as well as the respective standard deviation, are given in Table 1. The mean absolute

Table 1. Mean Temperature Deviations of Methods

	OH$_{\text{center}}$ (K)	IADS (K)	2-color (K)
$T_{\text{diff,H}_2\text{O}}$	2.89	0.07	1.61
STD $T_{\text{diff,H}_2\text{O}}$	1.22	0.85	1.16
$T_{\text{diff,EtOH}}$	0.51	0.10	1.26
STD $T_{\text{diff,H}_2\text{O}}$	1.60	1.15	3.73
$T_{\text{diff,EtOH-N}_2}$	1.46	1.03	3.25
STD $T_{\text{diff,EtOH-N}_2}$	1.32	1.14	3.06

temperature deviations of the methods OH$_{\text{center}}$ and IADS appear to have a significant advantage over the 2-color method for ethanol and the ethanol−nitrogen mixture. The IADS method should be the preferred one, providing at least 20% less standard deviation compared to the OH$_{\text{center}}$ method and performing superior for water. Furthermore, the relative thermal sensitivities at 433 K, calculated as $S_r = (\delta Q/\delta T)/Q$, where Q is the respective signal value, of the methods OH$_{\text{center}}$ and IADS for the respective systems water, ethanol, and ethanol−nitrogen are given in Table 2.

Table 2. Relative Thermal Sensitivities at 433 K

	$S_{\text{r,OHcenter}}$ (%)	$S_{\text{r,IADS}}$ (%)
H$_2$O	0.014 K^{-1}	0.597 K^{-1}
EtOH	0.037 K^{-1}	0.841 K^{-1}
EtOH−N$_2$	0.037 K^{-1}	0.801 K^{-1}

Pressure Dependence. The data shown so far comprise measurements performed at different pressures, assuming negligible pressure dependence of the spectra. To show that this assumption holds true, Figure 12 shows the respective correlation value for the methods OH$_{\text{center}}$ and IADS at a temperature of 433 K (approximate center of the investigated temperature interval) over pressure for the three systems water, pure ethanol, and ethanol−nitrogen. The OH$_{\text{center}}$ method shows a shift of $\bar{\nu}_{\text{center}}$ of 5 cm^{-1} from 0.5 to 25 MPa, converting to an error in calculated temperature T_{calc} of less than 10 K. This error adds to the standard deviation in the plots (see Figure 5, bottom). For pure ethanol, this error from 3 to 8 MPa also converts to less than 10 K, while no significant pressure dependence is found for ethanol−nitrogen with the OH$_{\text{center}}$ method. The IADS method exhibits no pressure
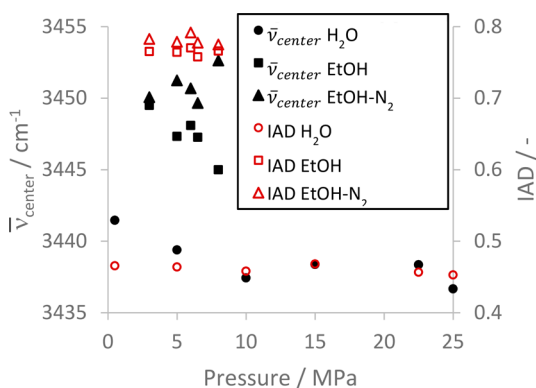
Figure 12. $\bar{\nu}_{center}$ (left axis) and IAD (right axis) over pressure for water, pure ethanol, and the ethanol−nitrogen mixture at 433 K.

dependence whatsoever due to the fact that each pressure set has its own reference spectrum taken at the respective system pressure, canceling out any pressure effects.

CONCLUSION

Four methods for the liquid phase temperature measurement with Raman spectroscopy in fluids developing hydrogen bonds were compared. To the first of our knowledge, this was done by covering the pressure range from slightly elevated pressures (0.5 MPa) to supercritical pressures with respect to ethanol and water and the accompanying temperature range from ambient temperature to phase transition or transition from liquid-like to gas-like supercritical state. It was shown that the IADS method is superior in pure fluids as well as mixtures, closely followed by the OH_{center} method. IADS is a mathematically simple approach and appears to be promising even in mixtures containing higher amounts of solvent. The methods are applicable throughout the liquid-like temperature range at supercritical pressures, where a sudden change in the shape of the Raman OH-band indicates the transition to the gas-like region. Concerning mixtures, the measurement approach is limited regardless of evaluation method to the persistence of a hydrogen bond network. With increasing dilution of the hydrogen bond developing compound, the sensitivity of the thus inhibited hydrogen bond network to temperature variations will decrease. Yet we could not detect significant negative impacts within the investigated ethanol−nitrogen mixture of up to 4 mol % nitrogen.

ASSOCIATED CONTENT

Ⓢ Supporting Information

The Supporting Information is available free of charge on the ACS Publications website at DOI: 10.1021/acs.analchem.8b04382.

    Equations for the functions fitted to the signal data over temperature figures of this work (PDF)

AUTHOR INFORMATION

Corresponding Author
*E-mail: andreas.braeuer@tu-freiberg.de.

ORCID Ⓘ
Andreas S. Braeuer: 0000-0002-7816-4027

Author Contributions
The manuscript was written through contributions of all authors.

REFERENCES
(1) Kim, M. M.; Giry, A.; Mastiani, M.; Rodrigues, G. O.; Reis, A.; Mandin, P. *Microelectron. Eng.* **2015**, *148*, 129−142.
(2) Childs, P. R. N.; Greenwood, J. R.; Long, C. A. *Rev. Sci. Instrum.* **2000**, *71*, 2959−2978.
(3) Eckbreth, A. C. *Laser Diagnostics for Combustion Temperature and Species*, 2nd ed.; Combustion Science and Technology Book Series; CRC Press: Boca Raton, 1996; Vol. 3.
(4) Liu, X.; Smith, M. E.; Tse, S. D. *Appl. Phys. B: Lasers Opt.* **2010**, *100*, 643−653.
(5) Braeuer, A.; Leipertz, A. *Appl. Opt.* **2009**, *48*, B57−B64.
(6) Bahr, L. A.; Fendt, P.; Pang, Y.; Karl, J.; Hammer, T.; Braeuer, A. S.; Will, S. *Opt. Lett.* **2018**, *43*, 4477−4480.
(7) Rabenstein, F.; Leipertz, A. *Appl. Opt.* **1998**, *37*, 4937−4943.
(8) Rabenstein, F.; Leipertz, A. *Appl. Opt.* **1997**, *36*, 6989−6996.
(9) Morawietz, T.; Marsalek, O.; Pattenaude, S. R.; Streacker, L. M.; Ben-Amotz, D.; Markland, T. E. *J. Phys. Chem. Lett.* **2018**, *9*, 851−857.
(10) Holzammer, C.; Finckenstein, A.; Will, S.; Braeuer, A. S. *J. Phys. Chem. B* **2016**, *120*, 2452−2459.
(11) Carey, D. M.; Korenowski, G. M. *J. Chem. Phys.* **1998**, *108*, 2669.
(12) Walrafen, G. E.; Fisher, M. R.; Hokmabadi, M. S.; Yang, W.-H. *J. Chem. Phys.* **1986**, *85*, 6970.
(13) Becucci, M.; Cavalieri, S.; Eramo, R.; Fini, L.; Materazzi, M. *Appl. Opt.* **1999**, *38*, 928−931.
(14) Smith, J. D.; Cappa, C. D.; Wilson, K. R.; Cohen, R. C.; Geissler, P. L.; Saykally, R. J. *Proc. Natl. Acad. Sci. U. S. A.* **2005**, *102*, 14171−14174.
(15) Buback, M.; Schulz, K. R. *J. Phys. Chem.* **1976**, *80*, 2478−2482.
(16) Müller, T.; Grünefeld, G.; Beushausen, V. *Appl. Phys. B: Lasers Opt.* **2000**, *70*, 155−158.
(17) Knauer, O. S.; Lang, M. C.; Braeuer, A.; Leipertz, A. *J. Raman Spectrosc.* **2011**, *42*, 195−200.
(18) Lednev, V. N.; Grishin, M. Y.; Pershin, S. M.; Bunkin, A. F. *Opt. Lett.* **2016**, *41*, 4625−4628.
(19) Risović, D.; Furić, K. *J. Raman Spectrosc.* **2005**, *36*, 771−776.
(20) Grimaldi, N.; Rojas, P. E.; Stehle, S.; Cordoba, A.; Schweins, R.; Sala, S.; Luelsdorf, S.; Piña, D.; Veciana, J.; Faraudo, J.; Triolo, A.; Braeuer, A. S.; Ventosa, N. *ACS Nano* **2017**, *11*, 10774−10784.
(21) Hankel, R. F.; Günther, A.; Wirth, K.-E.; Leipertz, A.; Braeuer, A. *Opt. Express* **2014**, *22*, 7962−7971.
(22) Holzammer, C.; Schicks, J. M.; Will, S.; Braeuer, A. S. *J. Phys. Chem. B* **2017**, *121*, 8330−8337.